

Cover Page



Universiteit Leiden



The handle <http://hdl.handle.net/1887/21936> holds various files of this Leiden University dissertation.

Author: Berg, Yascha Wilfred van den
Title: Tissue factor isoforms and cancer
Issue Date: 2013-10-08

Chapter 2 - Alternatively spliced tissue factor induces angiogenesis through integrin ligation

YW van den Berg, LG van den Hengel, HR Myers, O Ayachi, E Jordanova, W Ruf, CA Spek, PH Reitsma, VY Bogdanov, and HH Versteeg.

Proc Natl Acad Sci U S A. 2009 Nov 17;106(46):19497-502.

Abstract

The initiator of coagulation, full-length tissue factor (fTF), in complex with factor VIIa, influences angiogenesis through PAR-2. Recently, an alternatively spliced variant of TF (asTF) was discovered, in which part of the TF extracellular domain, the transmembrane and cytoplasmic domains are replaced by a unique C-terminus. Subcutaneous tumors produced by asTF-secreting cells revealed increased angiogenesis, but it has remained mechanistically unclear if and how angiogenesis is regulated by asTF. Here, we show that asTF enhances angiogenesis in matrigel plugs in mice whereas a soluble form of fTF only modestly enhanced angiogenesis. Furthermore, asTF dose-dependently upregulates angiogenesis *ex vivo* independent of PAR-2 or VIIa. Rather, asTF was found to ligate integrins resulting in down stream signaling. asTF- α V β 3 integrin interaction induced endothelial cell migration, whereas asTF-dependent formation of capillaries *in vitro* was dependent on α 6 β 1 integrin. Finally, asTF-dependent aortic sprouting was sensitive to β 1 and β 3 integrin blockade and a TF-antibody that disrupts asTF-integrin interaction. We conclude that asTF, unlike fTF, does not affect angiogenesis through PAR-dependent pathways but relies on integrin ligation. These findings implicate that asTF might be specifically targeted to prevent pathological angiogenesis.

Introduction

The development of blood vessels out of existing vessels, termed angiogenesis, occurs in embryonic development, wound healing and cancer¹. Angiogenesis depends on initial tip cell migration from the existing vessel, followed by migration of stalk cells, which divide and form a capillary² and the recruitment of pericytes which align the capillary. Angiogenesis is regulated by proteins such as vascular endothelial growth factor (VEGF), metalloproteinases and interleukin-8^{1;3;4}, but also depends on integrins. In particular β 1 and β 3-type integrins play a role in endothelial and pericyte migration as well as capillary formation^{5;6}.

Upon vessel damage, Tissue Factor (TF) together with bloodborne factor VIIa, generates factors Xa, thrombin and fibrin, yielding a hemostatic plug⁷. TF is indispensable for angiogenesis since TF-deficient embryos die *in utero*⁸. Moreover, TF affects tumor angiogenesis in colorectal cancer and breast cancer models, through TF:VIIa-dependent Protease-activated Receptor-2 (PAR-2) activation⁹⁻¹¹, resulting in expression of VEGF, IL-8 and MMP-7 and CXCL-1¹⁰⁻¹³. In addition, TF binds α 3 β 1 and α 6 β 1 integrins and disruption of this complex downregulates pro-angiogenic signaling and suppresses of tumor growth *in vivo*^{11;14}.

Recently, a TF isoform, asTF, which results from alternative splicing, was discovered, in which the transmembrane and cytoplasmic domains are replaced by a unique 40 amino acid C-terminal domain, rendering asTF soluble¹⁵. asTF incorporates in thrombi and asTF secreted by endothelium exhibits pro-coagulant activity. The precise role of asTF is controversial as some groups failed to detect asTF procoagulant activity¹⁵⁻¹⁷, however asTF is expressed in malignancies such as pancreatic and lung cancer^{18;19}. Hobbs et al. demonstrated that pancreatic cancer cells transfected to express asTF produce more blood vessels²⁰, but it remained mechanistically unclear if and how angiogenesis is regulated by asTF. One possibility is that asTF stimulates cancer cells to produce angiogenic factors, but it is also plausible that asTF enhances angiogenesis via paracrine stimulation of endothelial cells. Moreover, the role of VIIa, PAR-2 activation and downstream coagulation activation remained obscure.

In this study we report that asTF enhances angiogenesis *in vivo*, *ex vivo* and *in vitro* independent of downstream coagulation factors or activation of PAR-2, but dependent on $\alpha v\beta 3$ and $\alpha 6\beta 1$ integrin function.

Materials and methods

Materials- Matrigel, anti- $\alpha 3$ (P1B5), anti- $\alpha 6$ (GoH3), anti- $\beta 2$ (YFC118.3), anti- $\beta 3$ (B3A) and anti- $\alpha v\beta 3$ (LM609) were obtained from Millipore (Billerica, MA); Anti- $\beta 4$ (346-11) was from Abcam (Cambridge, UK). Recombinant mouse VEGF, pFAK and total FAK antibodies were purchased from Invitrogen (Carlsbad, CA); Recombinant factor VIIa and active site blocked VIIa (ASIS) were obtained from Novo Nordisk (Maalov, Denmark). Anti-integrin $\beta 1$ clone AIIIB2, anti-TF 10H10, 5G9, 6B4 and 9C3 mAb's were described before^{28;29}; pERK1/2 and total ERK1/2 antibodies were purchased from Cell Signaling Technologies (Danvers, MA). Anti-mouse $\beta 1$ (9EG7) and $\beta 3$ (2C9.G2) were from, BD Pharmingen (Franklin Lakes, NJ). Isopropyl- β -D-thiogalactopyranoside (IPTG) was obtained from Promega (Madison, WI). BugBuster protein extraction reagent and His-bind purification kit were obtained from Novagen (Madison, WI). Polymyxin B sulphate salt, FITC-labeled dextran and 3-[4,5-dimethylthiazol-2-yl]-2,5-diphenyl tetrazolium bromide (MTT) were obtained from Sigma (St. Louis, MO). SLIGRL was ordered from peptides international (Louisville, KY). Akt inhibitor IX and hiruding were purchased from Calbiochem (San Diego, CA). T75 Cell culture flasks and other cell culture disposables were purchased from Greiner Bio-One (Alphen a/d Rijn, the Netherlands). Images were captured using Motic Image Analysis Software™.

Animals- Male C57Bl/6 mice were obtained from Harlan Sprague-Dawley, Horst, The Netherlands and were maintained at the animal care facility of the Leiden University

Medical Center according to institutional guidelines. Animal procedures were carried out in compliance with Institutional Standards for Humane Care and Use of Laboratory Animals. The Animal Care and Use Committee of the Leiden University Center approved all experiments.

Cell culture- ECRF cells are immortalized endothelial cells that behave similar to primary HUVECs and were provided by Dr. Ruud Fontijn³⁰. All experiments involving endothelial cells were performed with this cell line, but key experiments were repeated using HUVECs. Pericytes (Applied Cell Biology Research Institute, Kirkland WA) were cultured with CS-C complete medium system, supplied with 10% serum. ECRF and HUVEC were cultured in Endothelial Growth Media (Lonza, Walkersville, MD) containing 2% serum. Culturing conditions were 37°C, 5% CO₂ and 95% humidity. Cells were typically passaged three times a week at 70-90% confluence. When appropriate, endothelial cells were adenovirally transduced to express TF and PAR-2 as described before³¹. Mouse embryonic endothelial cells (MEEC) were grown and passaged in DMEM, supplemented with 10% FCS. For inhibitor studies, cells were incubated with inhibitors for 20 min at the indicated concentrations, prior to the experiment.

Production of recombinant asTF- Recombinant asTF mature protein, with a 6X-His tag placed at its N-terminus, was produced in E. coli harboring a pTriEx3-Neo-asTF expression vector (Novagen, Madison, WI). Bacteria were cultured in Luria-Bertani (LB) medium containing 50 µg/ml ampicillin and 34 µg/ml chloramphenicol. asTF synthesis was induced in 1 L culture by adding 750 µM IPTG upon OD₆₀₀ of the culture reaching ~0.9. Following 16 hr incubation at 37°C, bacteria were pelleted and soluble asTF was purified from the cytosolic extract using BugBuster protein extraction reagent and His-bind purification kit (Novagen). Purity of the protein preparation was verified on SDS-PAGE gel using Coomassie Brilliant blue staining, and protein concentration determined using Bradford reagent (Bio-Rad). The preparation was dialyzed overnight in PBS, diluted 1:1 with sterile glycerol, and stored at -20°C for experiments. Eukaryotic asTF and soluble TF (sTF) were produced by transiently transfecting Baby Hamster Kidney (BHK) cells with expression vectors for asTF and sTF (pTriEx3 and pcDNA3.1 respectively). 6-wells plates containing BHK cells were transfected using Lipofectamine 2000 (Invitrogen, Carlsbad, CA) following the protocol of the supplier.

Proliferation assay- Cells were grown 30% confluent in 24-wells plates and serum starved for 5 hrs. Stimulant was added for 24 hrs and proliferation was measured using an MTT assay (a colorimetric assay in which a tetrazolium compound is bio-reduced by cells into a colored formazan product in direct proportion to the number of living cells in culture). In

brief, the cells were incubated with 0.5 mg/ml MTT for 30 min and converted MTT was extracted with isopropanol/0.04 N HCl. OD590 of the extract was measured using an ELISA-reader and survival was determined as a percentage of untreated cells at day 0.

Western Blotting- Cell lysates were loaded on SDS-page and transferred to PVDF membrane, blocked in 5% non-fat dry milk/TBST and incubated with primary antibodies O/N in blockbuffer. After extensive washing, the membranes were incubated with 1:2000 secondary antibodies conjugated to Horseradish Peroxidase. Bands were visualized with Supersignal WestFemto (Thermo Scientific, Rockford, IL). For detection of intratumoral asTF, lysed tumor material was subjected to SDS-page and transferred as described above. The membranes were blocked O/N in 3% non-fat milk/TBST and incubated with 3 µg/ml polyclonal anti-asTF for 2 h. After washing, membranes were incubated with secondary antibody and bands were visualized as described above. Bands were quantified using Scion Image (Scion Corporation, Frederick, MD) and compared to a concentration curve asTF on the same membrane.

Endothelial Cell Adhesion Assays- 96 well plates were coated with 50µg/ml asTF or 10% BSA as negative control. Uncoated areas were blocked with 10% BSA. 20,000 cells were seeded per well and plates were incubated at 37°C for 4 h. In some experiments, cells were preincubated with 50 µg/ml of integrin blocking antibodies. Photographs were taken and cells adopting a flattened morphology were counted. Data are shown as mean ± SD, n=4.

Cell Migration Assays- Cell migration was assessed using a transwell assay. 8.0 µm polycarbonate membrane transwell inserts (Corning-Costar; Corning Life Sciences, Corning NY) were coated with 1% gelatin or asTF (50 µg/ml). 25,000 cells were seeded per insert after a 20 min.pretreatment with integrin blocking mAb's, when appropriate. Cells were left to migrate for 5 h at 37°C, migrated cells were fixed and stained with crystal violet for 10 min. Cells were counted per field of 40x magnification.

In vitro capillary formation assay- 96-wells plates were coated with 50 µl matrigel, supplemented with asTF according to the experimental conditions. 20,000 endothelial cells were seeded after a 20 min. pretreatment with blocking antibodies when appropriate, left to form capillaries for 18 h (ECRF) or 6 h (HUVEC), and the length of tubular networks was measured.

Mouse Aortic Ring Assay- Mouse thoracic aortas were isolated and cleaned of surrounding tissue in serum free RPMI (Invitrogen, Carlsbad, CA) containing 50 u/ml penicillin and 50 µg/ml streptomycin. Dissected aortas were flushed, cut into equal segments, embedded in

matrigel and covered with EBM containing 2% serum and penicillin/streptomycin. Sprouts were counted on day 5. Aortas were also embedded in fibrin that was prepared by mixing 2 mg/ml fibrinogen with 0.1 U/ml thrombin. Aortas were then overlaid with medium containing 5 U/ml hirudin.

Matrigel plug Assay- 8-week-old C57Bl6 mice (n = 10 per group) were anaesthetized with isoflurane and injected subcutaneously into the flank with 0.5 ml ice-cold matrigel. Matrigel was either supplemented with 100 nM asTF or sTF in the presence/absence of 100 µg/ml 6B4, 50 ng/ml mouse recombinant VEGF or PBS. After 7 days, 150 µl FITC-Dextran (30 mg/ml) was injected into the tail vein. After 15 min. the animals were sacrificed, implants were extracted, fixed in 10% formalin and analyzed on a Leica MZ16 FA stereomicroscope.

Statistics- Data are mean +/- SD unless otherwise stated. Statistical analysis was performed using Student's t- test. p <0.05: *, p <0.01: **, p <0.001, ***

Results

asTF induces angiogenesis in vivo and ex vivo- To study a potential effect of asTF on angiogenesis, we evaluated the properties of recombinant asTF. Purified asTF migrated as a single band of ~26 kDa, corresponding to its predicted molecular weight, on SDS-PAGE (fig S1A). asTF exhibited pro-coagulant activity that was dependent on phospholipids, analogously to that of the native asTF secreted by human endothelial cells (not shown)¹⁷. The preparation reacted with a monoclonal antibody against the N-terminal part (9C3), but not with antibodies against the C-terminal part of full length TF (fTF) (10H10, 5G9) (fig S1B), demonstrating that the expressed protein was indeed asTF. Concordantly, similar immunoreactivity of these antibodies was observed after expression of asTF in eukaryotic cells (fig S1C).

Whether asTF induced angiogenesis was tested in a matrigel plug assay. Matrigel supplemented with asTF, VEGF or buffer control was injected into C57Bl/6 mice and angiogenesis was analyzed 7 days later. Both asTF and VEGF enhanced angiogenesis compared to the buffer control (fig 1A, S2A), showing that asTF can influence angiogenesis in the absence of tumor cells. Similar results were obtained in an *ex vivo* aortic sprouting model²¹ in which segmented aortas isolated from C57Bl/6 mice were implanted in matrigel containing asTF, VEGF or control buffer (fig 1B, S2B). Similar *ex vivo* experiments revealed that asTF concentration-dependently enhanced the formation of sprouts at concentrations as low as 1 nM. (fig 1C). Active site-blocked VIIa (ASIS) or hirudin, inhibitors to VIIa and thrombin respectively, did not inhibit asTF-dependent sprouting, indicating

that generation of coagulation proteases was not required (fig 1C). Moreover, adding asTF in combination with VIIa did not enhance aortic sprouting compared to asTF alone (fig 1D), supporting our finding that asTF induced angiogenesis independent of coagulation activation or ligand binding. asTF presence in the matrigel, but not in the media placed on top of the matrigel enhanced angiogenesis, suggesting that asTF presence in the extracellular matrix is required (fig 1E). Recombinant asTF was produced in *E. coli*, thus the presence of LPS contaminations could potentially influence sprout formation. However, inclusion of the LPS inhibitor polymyxin B did not influence aortic sprouting by asTF (fig 1F), and similar sprouting was observed in a serum free system (fig S3), a condition that does not allow for efficient LPS signaling²².

asTF-dependent angiogenesis is not dependent on PAR-2- Next we examined the mechanism behind asTF-induced angiogenesis. Endothelial cells under basal conditions express low levels of PAR-2, but these levels go up during angiogenesis¹⁰. TF in complex with VIIa was previously shown to promote PAR-2-dependent angiogenesis, presumably through activation of, among others, the MAP kinase signal transduction pathway. To study the influence of asTF on PAR-2 activation in endothelial cells, we used an endothelial cell line (ECRF), that was adenovirally transduced to express PAR-2, after which these cells were stimulated with asTF, VIIa, or the combination of asTF and VIIa. A truncated soluble form of fITF (sTF) in complex with VIIa and a PAR-2 agonist, SLIGRL, were used as positive controls. VIIa, asTF, or the combination of asTF and VIIa were not able to induce phosphorylation of MAP kinase, whereas VIIa in complex with sTF or SLIGRL induced strong phosphorylation within 10 min. (fig 2A). Similar results were observed in primary HUVEC cells (fig S4).

Since angiogenesis is dependent on endothelial cell proliferation, we also determined whether asTF induced proliferation in PAR-2 transduced cells. Fetal calf serum induced significant cell proliferation, but incubation with asTF, VIIa or the combination of asTF and VIIa were without effect (fig 2B,S4). In agreement, we found that aortic segments isolated from PAR-2^{-/-} mice displayed the same increase in asTF-dependent sprout formation as wild type segments, although basal sprouting in PAR-2^{-/-} segments was lower (fig 2C). Thus, the effect of asTF on angiogenesis is not dependent on VIIa-mediated activation of PAR-2. Importantly, the effect of asTF on sprouting was much larger than that observed using sTF, either in wild type aortas or PAR-2^{-/-} aortas (fig 2C), suggesting that asTF is the main TF isoform that mediates angiogenesis.

asTF binds endothelial integrins- Since fITF was previously shown to bind integrins, the effect of asTF on angiogenesis may be dependent on integrin ligation. To study this, tissue culture plates were coated with asTF and blocked with BSA, after which ECRF cells were

seeded. ECRF cells bound time-dependently to asTF-coated plates, whereas cells bound very poorly to BSA-only-treated plates (fig 3A). Cells bound to asTF displayed enhanced phosphorylation of Focal Adhesion Kinase (FAK), p42/p44 MAP kinase, p38 MAP kinase and Akt, events that are typical for integrin ligation (fig 3B). Inclusion of the LPS inhibitor polymyxin B did not influence cell adhesion to asTF (fig S5A). Depletion of asTF from our preparation using nickel-NTA abolished cell adhesion, whereas incubation of asTF preparations with non-nickel bound control beads still led to cell adhesion (fig S5B). Moreover, cell adhesion to asTF in the presence of the TF antibody 6B4, which interferes with TF-integrin binding¹⁴, was completely inhibited (fig 3C). Thus, enhancement of cell adhesion was entirely dependent on the presence of asTF. The use of sTF yielded similar results in this assay.

To identify the responsible integrins, ECRF cells were pre-incubated with blocking antibodies. β 2 or β 4 blockade did not inhibit cell adhesion to asTF, β 3 blockade modestly inhibited cell adhesion and β 1 blockade resulted in a 50% reduction of cell adhesion (fig 3D). The combination of β 1 and β 3 blockade reduced cell adhesion to basal levels. Similar results were obtained using a murine endothelial cell line (fig S5C), validating the use of human asTF in murine models such as the matrigel plug assay and the aortic ring assays. In conclusion, both β 1 and β 3 integrins bind to asTF to mediate cell adhesion.

asTF induces endothelial cell migration- During angiogenesis endothelial tip cells initially migrate out of the intima and subsequently endothelial cell proliferation and differentiation result in capillaries. We assessed whether asTF induced cell migration using a transwell assay. asTF induced a 4-fold upregulation in ECRF migration when present in the lower compartment, and cells appeared rounded (fig 4A). When the lower sides of transwells were coated with asTF, a 10-fold upregulation of cell migration was observed while cells displayed a flattened morphology.

Pericytes also contribute to angiogenesis. We found that asTF did not facilitate pericyte migration whereas a mix of extracellular matrix proteins optimized for pericyte binding supported potent migration (fig 4B). Therefore, asTF does not induce pericyte migration, but selectively leads to migration of endothelial cells. Interestingly, endothelial migration was reduced on sTF when compared to asTF, potentially explaining the lower angiogenic potential of sTF (fig 4C).

The identity of integrins involved in asTF-enhanced migration was determined with integrin-blocking antibodies. β 1, β 2 and β blocking antibodies, as well as a control antibody, were unsuccessful in blocking migration, but β 3 blockade fully inhibited migration (fig 4D). An $\alpha\beta$ 3 blocking antibody (LM609) also blocked asTF-dependent

migration, demonstrating that $\alpha\beta3$ is required for asTF-dependent migration (fig 4E). Similarly, $\alpha\beta3$ blockade inhibited migration of primary HUVECs (fig S6). It is important to note that $\alpha\beta3$ integrin blockade by LM609 induces apoptosis in endothelial cells²³, which may be responsible for the inhibiting effect on asTF-induced migration, but apoptosis or impaired endothelial cell migration on collagen I after LM609 treatment was not observed (not shown). PM did not affect migration, demonstrating that possible traces of LPS did not contribute to this effect (fig 4E).

To investigate the signal transduction pathways involved in asTF-dependent migration we pre-incubated cells with specific kinase inhibitors. The p38 MAP kinase inhibitor SB203580 and the PI3 kinase inhibitor LY294002, but not the p42/p44 MAP kinase inhibitor, completely abolished migration (fig 4F). An Akt inhibitor only partially inhibited asTF-dependent migration (fig 4G), suggesting that PI3-kinase acts through Akt-dependent and independent pathways.

asTF enhances endothelial capillary formation- Next, we determined asTF's potential to support capillary formation by seeding ECRF cells on matrigel supplemented with asTF or control buffer. The presence of asTF enhanced the formation of capillaries 2.5-fold (fig 5A,B). When asTF was added to the medium, capillary formation was inhibited, presumably by binding and blocking of integrins that are required for capillary formation on matrigel. Surprisingly, $\beta1$ but not $\beta3$ blockade inhibited capillary formation to sub-basal levels in ECRF and primary HUVECs (fig 5B,S7). Apparently, endothelial cell migration and capillary formation induced by asTF were dependent on different integrin heterodimers. Blockade of $\alpha3$ and $\alpha6$ integrin subunits that were previously shown to interact with flITF 10 was also tested. Integrin $\alpha6$ blockade inhibited asTF-induced capillary formation to sub-basal levels (fig 5C). In contrast, $\alpha3$ blockade modestly inhibited capillary formation, suggesting that $\alpha3$ integrins are relatively unimportant for this process.

Matrigel primarily consists of collagen and laminin, thus $\alpha3$ and $\alpha6$ may also function in the attachment of cells to matrigel. To verify whether the inhibition of capillary formation by $\alpha3$ and $\alpha6$ blockade was due to diminished adhesion to asTF, we tested $\alpha3$ and $\alpha6$ blockade on cell adhesion to asTF. $\alpha6$, but not $\alpha3$, blockade partially inhibited cell binding to asTF (fig 5D). Cell adhesion was reduced to basal levels upon inclusion of a $\alpha3$ blocking antibody, supporting the conclusion that endothelial cells employ different integrin heterodimers, namely $\alpha6\beta1$ and $\alpha\beta3$, but only require $\alpha6\beta1$ integrin for asTF-induced capillary formation. Preincubation of ECRF cells with SB203580, LY294002 and PD98059 showed that asTF-induced capillary formation was dependent on p42/p44 MAP kinase and PI3-kinase action, but not the promigratory p38 MAP kinase cascade (fig 6E), demonstrating that distinct integrin-dependent pathways are involved in asTF-dependent

migration and capillary formation. In support of that, cells allowed to form capillaries on matrigel supplemented with asTF showed higher levels of p42/p44 and Akt, but not p38 phosphorylation.

Similar to what was observed in aortic sprouting experiments, Vllai, hirudin and polymyxin B did not influence capillary formation (fig 5C,E), demonstrating that asTF-dependent capillary formation was not dependent on coagulation activation and/or LPS contamination.

asTF-enhanced aortic sprouting is dependent on integrins- We next assessed the relative contributions of $\beta 1$ and $\beta 3$ integrins to asTF-dependent sprout formation in matrigel with blocking integrin antibodies. Blockade of $\beta 1$ inhibited basal sprouting and asTF-induced sprouting to the same levels (fig 6A), suggesting that both matrigel and asTF ligation of integrins was inhibited. Blockade of $\beta 3$ did not affect basal sprouting, but reduced asTF-dependent sprouting to basal levels. This is expected because matrigel contains relatively little $\beta 3$ -ligating matrix proteins. 6B4, which inhibits asTF-integrin interaction, similarly reduced asTF-dependent aortic sprouting (fig 6B).

asTF was previously found in thrombi and could therefore potentiate angiogenesis in a fibrin matrix. asTF dose-dependently upregulated sprouting similarly to that observed in matrigel (fig 6C). sTF similarly enhanced sprouting, but at much higher concentrations. Inclusion of 6B4 and blockade of $\beta 1$ and $\beta 3$ integrins led to inhibition of asTF-dependent sprouting (fig 6D). In contrast to what was observed in matrigel, $\beta 3$ but not $\beta 1$ blockade inhibited to subbasal levels, reflecting the requirement of $\beta 3$ integrin activation by fibrin. The asTF/integrin-blocking antibody 6B4 reduced vessel formation *in vivo*, and although soluble TF modestly induced vessel formation, 6B4 did not have an effect (fig 6E). Thus, integrins are instrumental in asTF-dependent sprouting in matrigel and fibrin and *in vivo* angiogenesis.

Intratumoral asTF concentrations- To test whether asTF concentrations that induce angiogenesis are pathologically relevant, we assessed intratumoral asTF concentrations in a set of cervical tumors. We chose cervical cancer since high levels of asTF mRNA were observed in tumors from 7 patients (fig 7A). 10 tumors were grinded and analysed for asTF expression on Western Blot using a specific asTF antibody. Bands were quantified and compared with an asTF concentration curve. All but one of these tumors contained asTF concentrations that fell within the range that induces angiogenesis (fig 7B). Thus asTF-induced angiogenesis is pathologically relevant.

Discussion

Here, we show that recombinant asTF induces angiogenesis in a matrigel plug assay and aortic sprouting in matrigel and fibrin. asTF induced angiogenesis in a VIIa/PAR-2-independent manner but acted through ligation of $\beta 1$ and $\beta 3$ integrins, at concentrations as low as 1 nM. asTF-induced endothelial cell migration and capillary formation was dependent on $\alpha v\beta 3$ and $\alpha 6\beta 1$ respectively. Our conclusion that asTF binds integrins is based on the following; i) endothelial cell adhesion to asTF as well as asTF-induced capillary formation and aortic sprouting were potently inhibited by integrin blocking antibodies, ii) inclusion of asTF in the medium blocked formation of capillaries, presumably by blocking integrins and iii) an antibody that inhibits TF-integrin interaction similarly inhibited sprouting and *in vivo* angiogenesis. Only the combination of $\beta 1$ and $\beta 3$ integrin blocking antibodies completely abrogated asTF-dependent cell adhesion, thus both $\beta 1$ and $\beta 3$ integrin appear to physically bind to asTF. This distinguishes asTF from matrigel and fibrin which predominantly activate $\beta 1$ and $\beta 3$ integrins respectively. Although the importance of other integrin ligands e.g. fibronectin and vitronectin cannot formally be excluded, they are not constituents of tumor extracellular matrix (Matrigel) or the provisional angiogenic fibrin matrix, and therefore play no role in our model. Endothelial cell migration was dependent on $\alpha v\beta 3$ integrin, p38 MAP kinase and PI3-kinase, whereas capillary formation was dependent on $\alpha 6\beta 1$, p42/p44 MAP kinase and PI3-kinase. It is noteworthy that tip cell migration and capillary formation represent different stages of angiogenesis and involves different integrins²⁴. Concordantly, $\alpha v\beta 3$ ligation results in directional migration, whereas $\beta 1$ ligation induces non-directional migration that is likely to be more important for capillary formation²⁵. In wound healing, $\alpha v\beta 3$ is focally expressed at the tips of invading capillary sprouts whereas $\beta 1$ integrins are widely expressed on the entire capillary²⁶. It appears that asTF-driven migration through $\alpha v\beta 3$ integrin mimics endothelial tip cell migration, whereas $\beta 1$ -dependent capillary formation through $\alpha 6\beta 1$ recapitulates the formation of vessels from non-tip cell endothelial cells through migration and differentiation. In aortic sprouting assays, which combine these features, asTF-induced angiogenesis was indeed sensitive to both $\beta 1$ and $\beta 3$ blockade.

fITF on tumor cells has also been shown to induce angiogenesis, but in a mechanistically different manner. Like asTF, fITF interacts with integrins, but rather than serving as receptors to TF, integrin $\alpha 3\beta 1$ and $\alpha 6\beta 1$ control fITF-VIIa signaling via PAR-2 10. The fact that fITF is membrane bound and binds integrins expressed on the same cell surface, whereas asTF is a soluble protein capable of being deposited into the extracellular matrix, i.e. at sites not accessible to fITF, may lie at the basis of this. fITF and asTF may thus bind

integrins in distinct orientations, determining specificity of integrins for the different forms of TF. Our work, showing a lack of asTF- $\alpha 3\beta 1$ integrin interaction, supports such a concept.

Another important finding is that asTF is a much more potent inducer of angiogenesis than a truncated form of flTF (sTF), presumably because asTF is more pro-migratory than sTF, making extracellular asTF the principal candidate to engage in integrin-dependent angiogenesis. The underlying basis may be differential integrin activation by asTF and flTF. Indeed, asTF differs from flTF such that asTF displays decreased affinity for VII (unpublished data) and lacks a functional X binding site due to the altered C-module.

In our experiments, asTF induced angiogenesis at concentrations as low as 1 nM. Interestingly, in a panel of 10 cervical tumors, we found that 9 out of 10 tumors contained asTF levels that were in the range within which asTF is proangiogenic, making asTF a potential keyplayer in tumor angiogenesis. In agreement, asTF expression has been found in pancreatic cell lines¹⁸, squamous cell carcinoma of the lung²⁷ advanced stages of non-small cell lung cancer¹⁹ and it appears to drive tumor growth in xenograft models²⁰. It remains controversial whether asTF displays coagulant activity and whether it is secreted by cells¹⁶. Regardless of whether asTF is procoagulant, we did not observe extensive thrombus formation in our *in vivo* experiments using either asTF or sTF, ruling out that these proteins induce thrombus formation in newly formed vessels. Szotowski et al.¹⁷ showed that asTF can be secreted after appropriate stimulation and asTF is found in plasma of healthy volunteers, making up approximately 30% of the total blood-borne TF pool¹⁵. Although the cue to asTF secretion in tumors remains to be identified, hypoxia or tumor-expressed cytokines may contribute to this phenomenon.

Authorship contributions

Y.v.d.B. designed and performed experiments, analyzed data, and wrote the manuscript. L.v.d.H., H.R.M., O.A. and E.J. performed experiments. W.R., C.A.S. and V.Y.B. provided reagents and resources, P.H.R. wrote the manuscript, H.H.V. supervised the project and wrote the manuscript.

Acknowledgements

We acknowledge Lars C. Petersen (Novo Nordisk, Maalov, Denmark) for the gift of VIIai. HHV is supported by The Netherlands Scientific Organisation (grant nr 916.76.012), WR is supported by NIH (HL060742 and HL016411). VYB is supported by NIH (grant K01 DK065752). Conflict of interest disclosure: None

Reference List

1. Carmeliet P. Angiogenesis in life, disease and medicine. *Nature* 2005;438:932-936.
2. Holderfield MT, Hughes CC. Crosstalk between vascular endothelial growth factor, notch, and transforming growth factor-beta in vascular morphogenesis. *Circ.Res.* 2008;102:637-652.
3. Rundhaug JE. Matrix metalloproteinases and angiogenesis. *J.Cell Mol.Med.* 2005;9:267-285.
4. Li A, Dubey S, Varney ML, Dave BJ, Singh RK. IL-8 directly enhanced endothelial cell survival, proliferation, and matrix metalloproteinases production and regulated angiogenesis. *J.Immunol.* 2003;170:3369-3376.
5. Brooks PC, Clark RA, Cheres DA. Requirement of vascular integrin alpha v beta 3 for angiogenesis. *Science* 1994;264:569-571.
6. Bloch W, Forsberg E, Lentini S et al. Beta 1 integrin is essential for teratoma growth and angiogenesis. *J.Cell Biol.* 1997;139:265-278.
7. Versteeg HH, Ruf W. Emerging insights in tissue factor-dependent signaling events. *Semin.Thromb.Hemost.* 2006;32:24-32.
8. Carmeliet P, Mackman N, Moons L et al. Role of tissue factor in embryonic blood vessel development. *Nature* 1996;383:73-75.
9. Yu JL, May L, Lhotak V et al. Oncogenic events regulate tissue factor expression in colorectal cancer cells: implications for tumor progression and angiogenesis. *Blood* 2005;105:1734-1741.
10. Versteeg HH, Schaffner F, Kerver M et al. Inhibition of tissue factor signaling suppresses tumor growth. *Blood* 2007
11. Versteeg HH, Schaffner F, Kerver M et al. Protease-activated receptor (PAR) 2, but not PAR1, signaling promotes the development of mammary adenocarcinoma in polyoma middle T mice. *Cancer Res.* 2008;68:7219-7227.
12. Milsom CC, Yu JL, Mackman N et al. Tissue factor regulation by epidermal growth factor receptor and epithelial-to-mesenchymal transitions: effect on tumor initiation and angiogenesis. *Cancer Res.* 2008;68:10068-10076.
13. Zhang JQ, Wan YL, Liu YC et al. The FVIIa-tissue factor complex induces the expression of MMP7 in LOVO cells in vitro. *Int.J.Colorectal Dis.* 2008;23:971-978.
14. Dorfleutner A, Hintermann E, Tarui T, Takada Y, Ruf W. Cross-talk of integrin alpha3beta1 and tissue factor in cell migration. *Mol.Biol.Cell* 2004;15:4416-4425.
15. Bogdanov VY, Balasubramanian V, Hathcock J et al. Alternatively spliced human tissue factor: a circulating, soluble, thrombogenic protein. *Nat.Med.* 2003;9:458-462.
16. Censarek P, Bobbe A, Grandoch M, Schror K, Weber AA. Alternatively spliced human tissue factor (asHTF) is not pro-coagulant. *Thromb.Haemost.* 2007;97:11-14.
17. Szotowski B, Antoniak S, Rauch U. Alternatively spliced tissue factor: a previously unknown piece in the puzzle of hemostasis. *Trends Cardiovasc.Med.* 2006;16:177-182.
18. Haas SL, Jesnowski R, Steiner M et al. Expression of tissue factor in pancreatic adenocarcinoma is associated with activation of coagulation. *World J.Gastroenterol.* 2006;12:4843-4849.
19. Goldin-Lang P, Tran QV, Fichtner I et al. Tissue factor expression pattern in human non-small cell lung cancer tissues indicate increased blood thrombogenicity and tumor metastasis. *Oncol.Rep.* 2008;20:123-128.
20. Hobbs JE, Zakarija A, Cundiff DL et al. Alternatively spliced human tissue factor promotes tumor growth and angiogenesis in a pancreatic cancer tumor model. *Thromb.Res.* 2007;120 Suppl 2:S13-S21.
21. Masson V, V, Devy L, Grignet-Debrus C et al. Mouse Aortic Ring Assay: A New Approach of the Molecular Genetics of Angiogenesis. *Biol.Proced.Online.* 2002;4:24-31.
22. Wright SD, Ramos RA, Tobias PS, Ulevitch RJ, Mathison JC. CD14, a receptor for complexes of lipopolysaccharide (LPS) and LPS binding protein. *Science* 1990;249:1431-1433.

23. Kuzuya M, Satake S, Ramos MA et al. Induction of apoptotic cell death in vascular endothelial cells cultured in three-dimensional collagen lattice. *Exp.Cell Res.* 1999;248:498-508.
24. Von Offenbergn SN, Cummins PM, Cotter EJ et al. Cyclic strain-mediated regulation of vascular endothelial cell migration and tube formation. *Biochem.Biophys.Res.Comm.* 2005;329:573-582.
25. Danen EH, Sonneveld P, Brakebusch C, Fassler R, Sonnenberg A. The fibronectin-binding integrins alpha5beta1 and alphavbeta3 differentially modulate RhoA-GTP loading, organization of cell matrix adhesions, and fibronectin fibrillogenesis. *J.Cell Biol.* 2002;159:1071-1086.
26. Clark RA, Tonnesen MG, Gailit J, Cheresch DA. Transient functional expression of alphaVbeta 3 on vascular cells during wound repair. *Am.J.Pathol.* 1996;148:1407-1421.
27. Rauch U, Antoniak S, Boots M et al. Association of tissue-factor upregulation in squamous-cell carcinoma of the lung with increased tissue factor in circulating blood. *Lancet Oncol.* 2005;6:254.
28. Versteeg HH, Schaffner F, Kerver M et al. Inhibition of tissue factor signaling suppresses tumor growth. *Blood* 2008;111:190-199.
29. Dorfleutner A, Hintermann E, Tarui T, Takada Y, Ruf W. Crosstalk of integrin a3b1 and tissue factor in cell migration. *Mol.Biol.Cell* 2004;15:4416-4425.
30. Fontijn R, Hop C, Brinkman HJ et al. Maintenance of vascular endothelial cell-specific properties after immortalization with an amphotrophic replication-deficient retrovirus containing human papilloma virus 16 E6/E7 DNA. *Exp.Cell Res.* 1995;216:199-207.
31. Dorfleutner A, Ruf W. Regulation of tissue factor cytoplasmic domain phosphorylation by palmitoylation. *Blood* 2003;102:3998-4005.

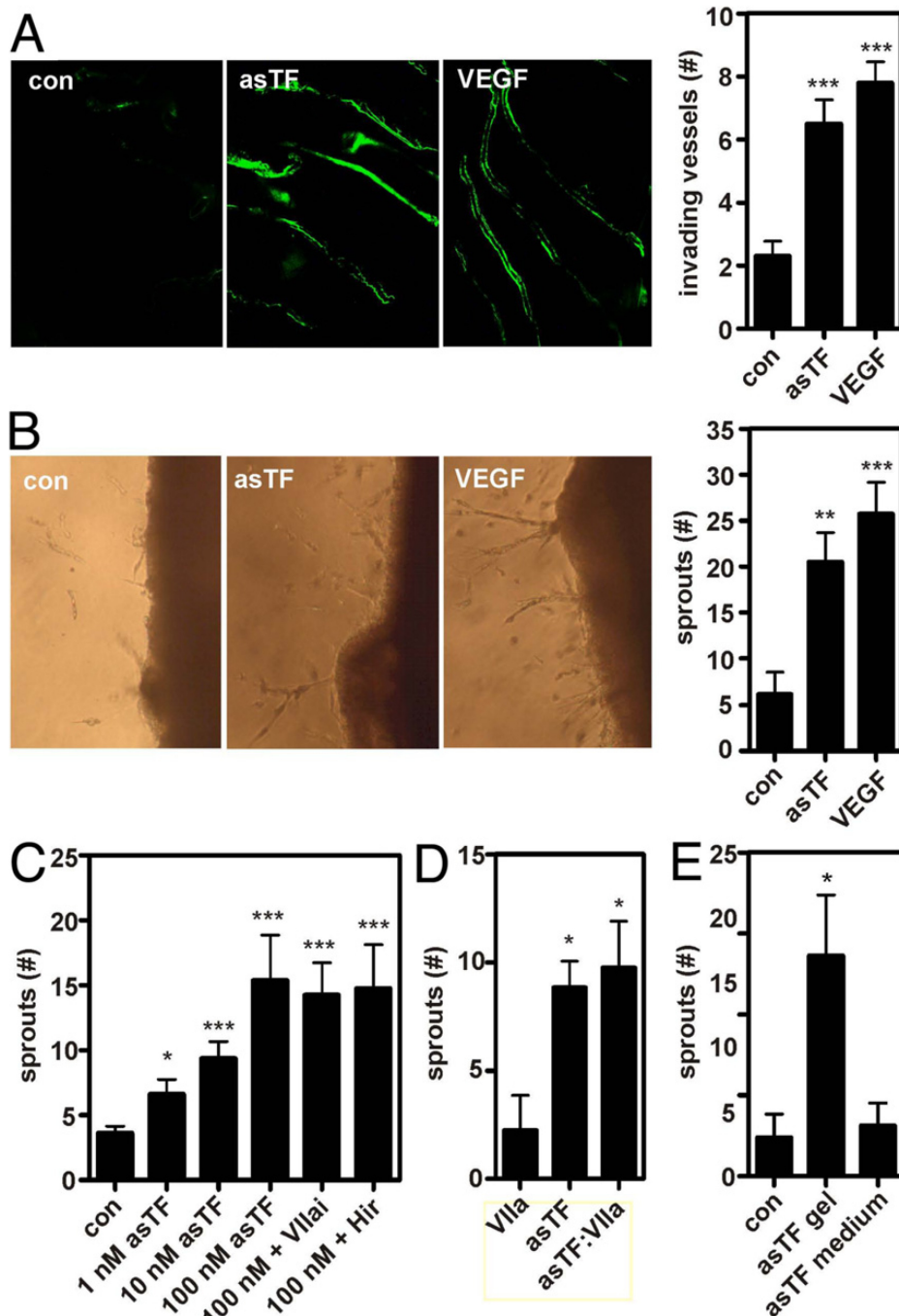


Figure 1. asTF induces angiogenesis *in vivo* and *ex vivo*. (A) Matrigel containing 100 nM asTF, 50 ng/ml VEGF or buffer control was injected subcutaneously into mice. FITC-dextran was tail vein-injected prior to sacrifice. Extracted plugs were examined and the number of invading vessels was counted ($n=10\pm\text{SEM}$). (B) Aortic segments from C57Bl/6 mice were implanted into matrigel supplemented with solvent control, asTF or VEGF. Sprouts were counted on day 5 ($n=8\pm\text{SEM}$). (C) Aortic segments in matrigel supplemented with solvent control or various concentrations of asTF. The coagulation inhibitors VIIai (100 nM) or hirudin (500 nM) were included in some of the conditions. (D) Aortic segments in matrigel supplemented with 100 nM VIIa, 100 nM asTF, or the combination of asTF and VIIa. (E) Sprouting occurs in asTF-containing matrigel, but not when media overlying the matrigel contains asTF. (F) The LPS-inhibitor Polymyxin B (PM; 50 $\mu\text{g}/\text{ml}$) does not inhibit asTF-dependent sprouting.

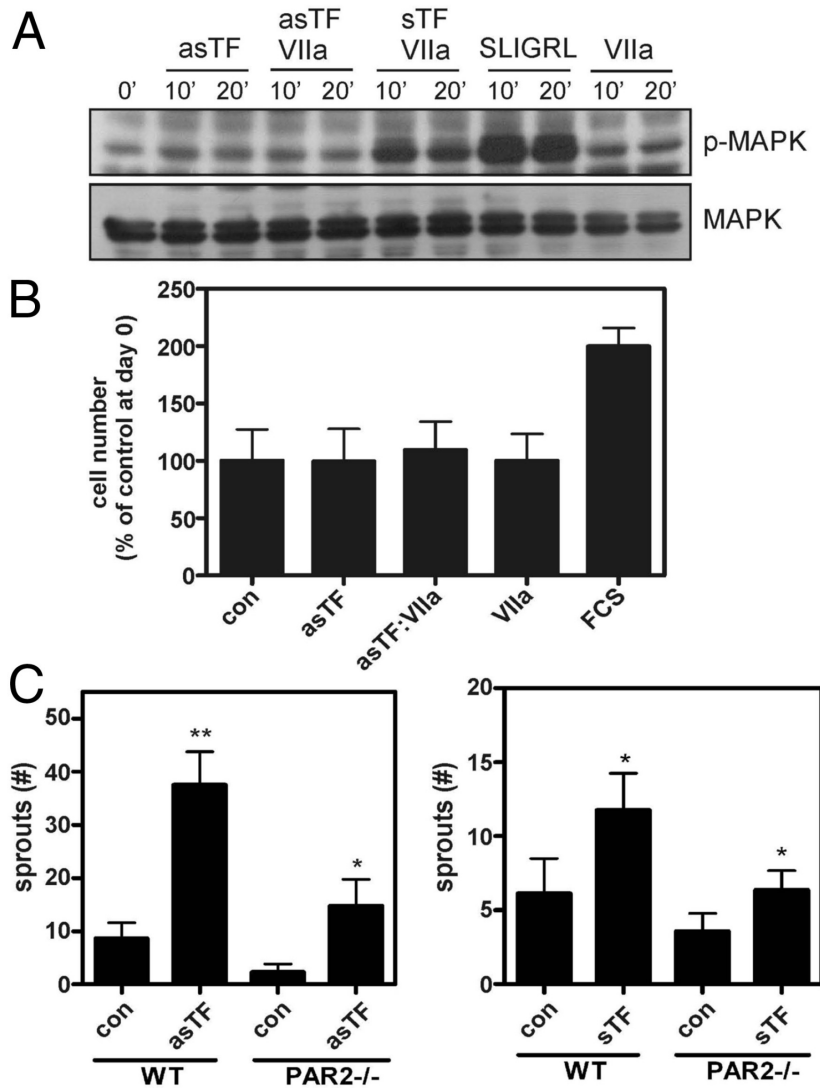


Figure 2. asTF does not activate PAR-2. (A) PAR-2-expressing ECRF cells were stimulated with 100 nM asTF ± 100 nM VIIa, VIIa alone, 100 nM truncated flTF + VIIa, or SLIGRL (100 μM). MAPK phosphorylation was determined by Western Blotting. (B) Cells were serum starved and stimulated with asTF ± VIIa, VIIa alone, or 15% FCS. Cell proliferation was assessed using MTT assays. (C) Aortic segments from wild type or PAR2^{-/-} C57Bl/6 mice were implanted in matrigel supplemented with solvent control, asTF or sTF and the number of sprouts was determined as described before.

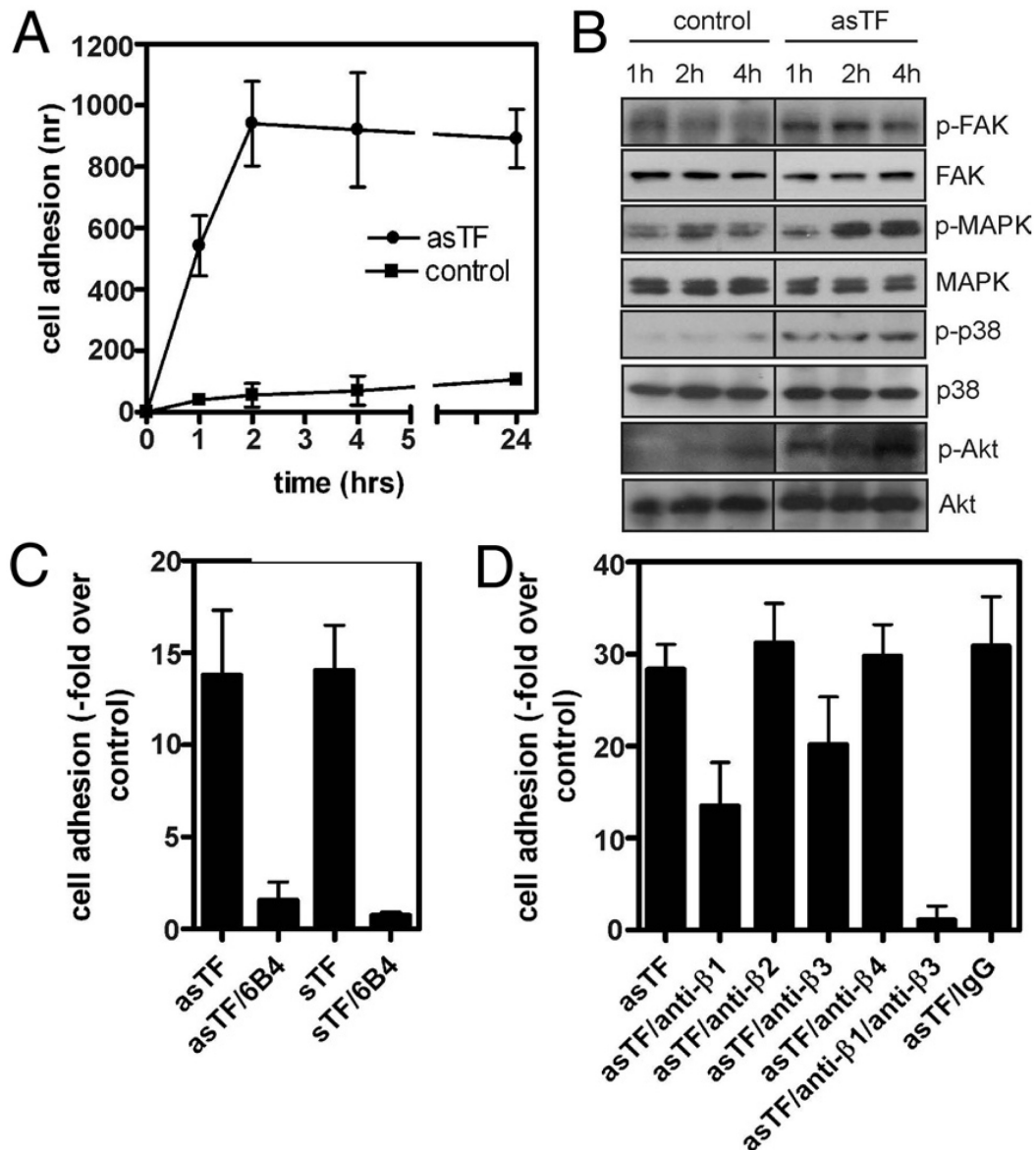


Figure 3. asTF binds endothelial cell integrins. (A) Cells were seeded on BSA- or asTF-coated culture wells and adhered cells were counted at the indicated times. (B) Cells were left to adhere to BSA- or asTF-coated wells for the indicated times, lysed, and the lysates were checked for FAK, p42/22 MAPK, p38 MAPK and c-Akt phosphorylation on Western Blot. Total levels of these proteins were assessed to verify equal loading. (C) Culture wells were coated with 50 $\mu\text{g}/\text{ml}$ asTF or sTF and cell adhesion was assayed in the absence/presence of 100 $\mu\text{g}/\text{ml}$ 6B4. (D) Endothelial cells were preincubated with integrin-blocking antibodies and seeded onto BSA- or asTF-coated wells. Adhered cells were counted.

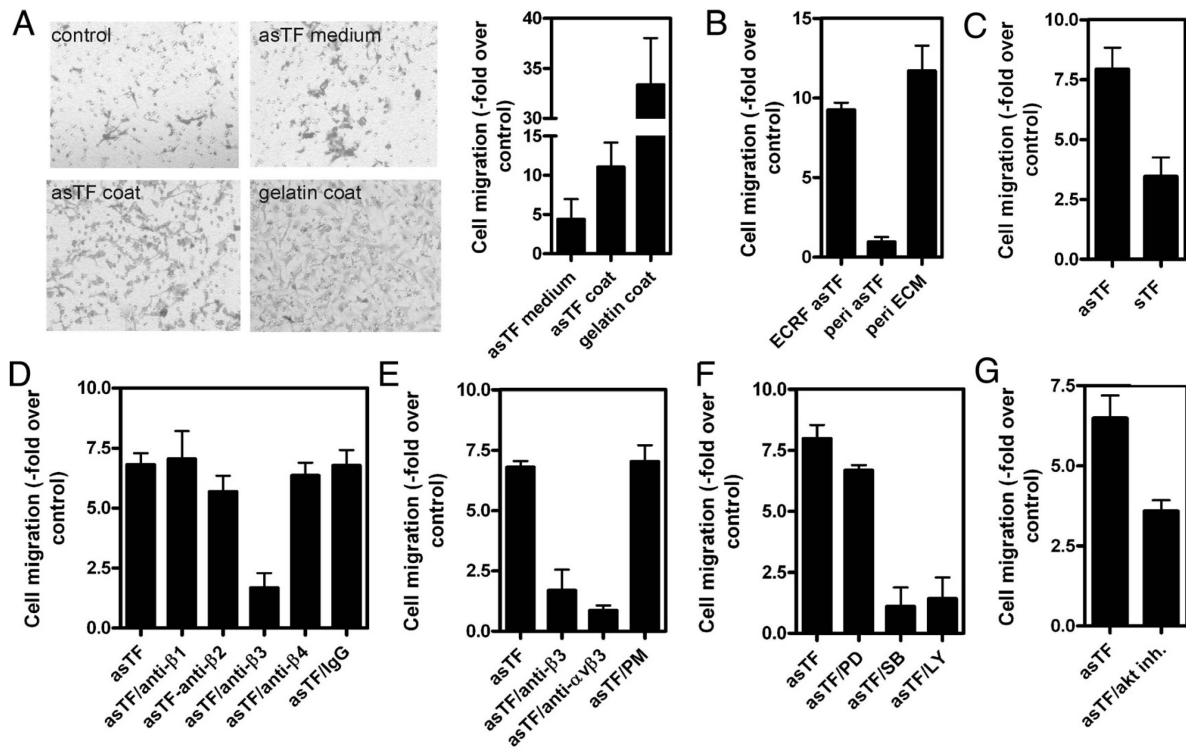


Figure 4. asTF induces $\alpha v \beta 3$ -dependent endothelial cell migration. (A) Transwell inserts were coated with BSA (negative control), 50 $\mu\text{g}/\text{ml}$ asTF or 1% gelatin (positive control). Endothelial cells were left to migrate for 5 h. Cells were also seeded in uncoated inserts and migration was induced by placing 100 nM asTF into the lower well. Note the rounded-up cell morphology of cells migrating towards a gradient of asTF versus the flattened morphology of cells migrating through asTF-coated inserts. The graph on the right shows a quantification of these results ($n=9$). (B) Pericytes were seeded into asTF-coated inserts or inserts coated with a pericyte extracellular matrix protein mix (Cell Systems) and left to migrate for 5 h. (C) Effect of asTF versus sTF coating on migration of ECRF cells. (D) Endothelial cells were preincubated with β integrin-blocking antibodies and seeded into asTF-coated transwell inserts. Migration was assessed as described above. (E) Endothelial cells were preincubated with $\alpha 3$ or $\alpha v \beta 3$ -blocking antibodies. asTF-induced cell migration was assessed as described before. Inclusion of PM in the assay did not inhibit migration. (F) Effects of MAPK pathway inhibitor PD98059 (20 μM), p38 MAPK inhibitor SB203580 (10 μM) or the PI-3 kinase inhibitor LY294002 (10 μM) on asTF-induced migration. (G) Effect of c-Akt inhibitor (10 μM) on asTF-induced migration.

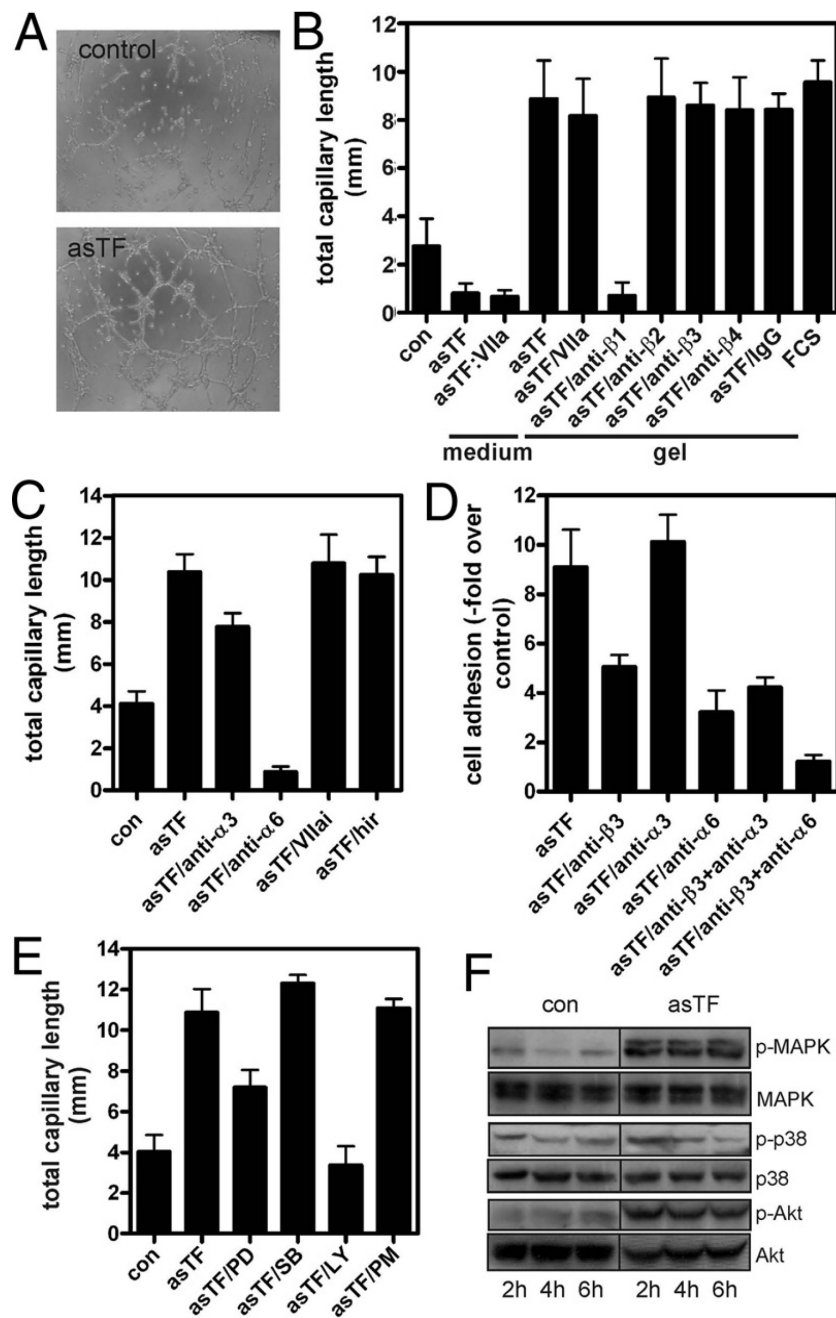


Figure 5. asTF enhances $\alpha6\beta1$ -dependent endothelial capillary formation. (A) Endothelial cells were seeded on matrigel supplemented with solvent control or 100 nM asTF. Photographs were made after O/N incubation. (B) Cells were seeded on matrigel containing solvent control or asTF. Alternatively, asTF was added to the medium containing the cells and the mix was added onto a matrigel layer without asTF. Cells were also preincubated with β integrin blocking antibodies and seeded onto asTF-containing matrigel. Total capillary length was quantified. (C) Cells were preincubated with $\alpha3$ or $\alpha6$ -blocking antibodies and seeded onto asTF-containing matrigel. Non-treated cells were also seeded onto asTF-containing matrigel in the presence of Vlla or hirudin. (D) Cells were preincubated with $\alpha3$ or $\alpha6$ -blocking antibodies in the presence or absence of $\beta3$ -blocking antibody before seeding of cells onto immobilized asTF. Adhered cells were counted after 4 h. (E) Effect of PD98059, SB203580 or LY294002 on asTF-induced capillary formation. (F) asTF-dependent phosphorylation of MAPK, p38 and Akt in capillary-forming endothelial cells. Cells were left to form capillaries for the times indicated on matrigel in the presence/absence of 100 nM asTF.

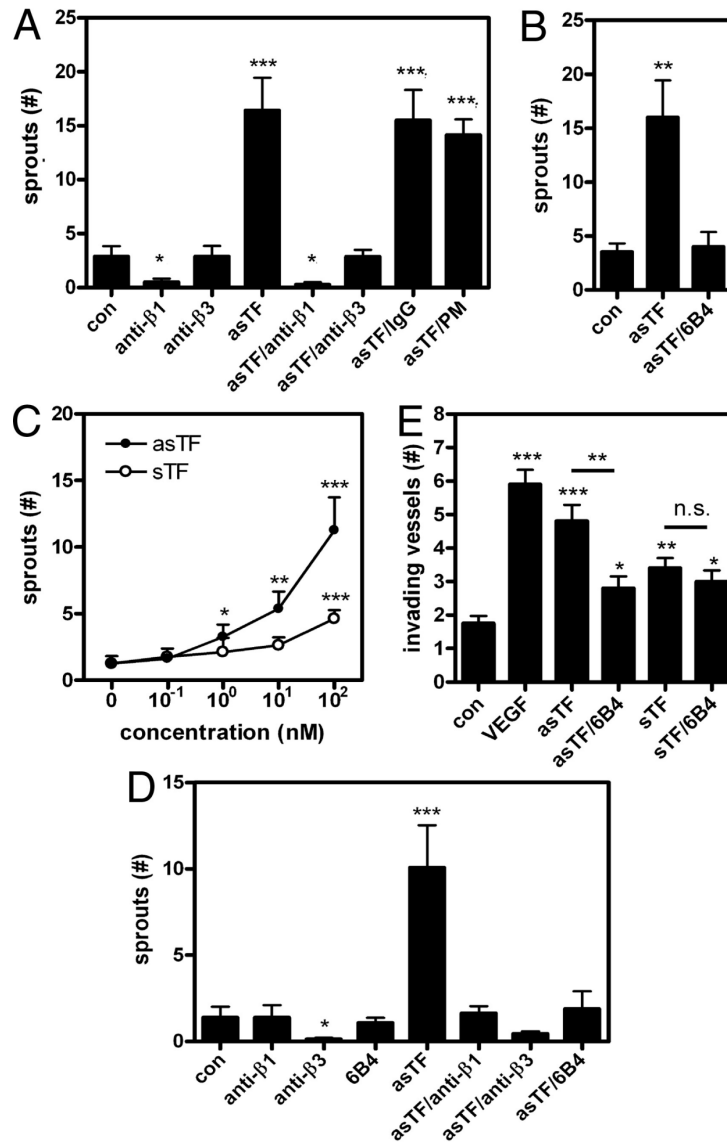


Figure 6. asTF induces integrin-dependent angiogenesis *in vivo* and *ex vivo*. (A) Wild type aortic segments were implanted in solvent control-containing matrigel or asTF-containing matrigel. Murine β 1 or β 3-blocking antibodies were added to the matrigel. The number of sprouts was determined as described before. Preincubation of aortas with these antibodies prior to implantation, or adding the antibodies to the medium on top of the segment-containing matrigel plugs gave similar results (not shown). (B) Wild type aortic segments were implanted in solvent control-containing matrigel or matrigel containing 6B4-preincubated (100 μ g/ml) asTF. (C) Wild type aortic segments in fibrin supplemented with various concentrations of asTF or sTF. (D) Wild type aortic segments in fibrin \pm 100 nM asTF, in the presence/absence of 50 μ g/ml integrin-blocking antibodies or 100 μ g/ml 6B4. (E) *in vivo* matrigel plug assay; matrigel was supplemented with control buffer VEGF, asTF or sTF. asTF and sTF were also preincubated with 100 μ g/ml 6B4 before addition to the matrigel. Vessels were counted as described above.

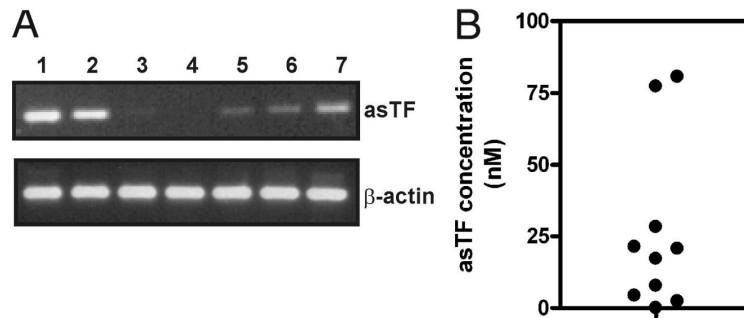


Figure 7. Cervical tumors express high levels of asTF. (A) mRNA obtained from 7 cervical tumors was subjected to RT-PCR using asTF- and β -actin-specific primers. (B) 10 cervical tumors were grinded and taken up in sample buffer. Lysates were analyzed for asTF expression on Western Blot and asTF bands were quantified using an asTF concentration curve.

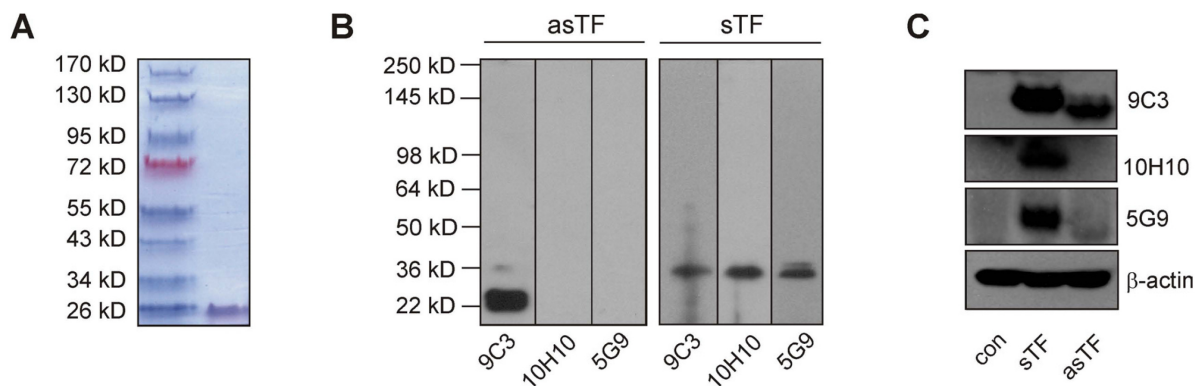


Fig S1 Expression of recombinant asTF. (A) asTF was expressed in *E. coli* and purified. asTF was loaded on SDS-PAGE and stained with Coomassie. (B) Reactivity of 10 ng asTF or soluble TF with the N-terminal specific flTF antibody 9C3 and the C-terminal flTF specific antibodies 10H10 and 5G9 on Western Blot. (C) Reactivity of eukaryotic soluble TF and asTF with 9C3, 10H10 and 5G9. BHK cells were transiently transfected, lysed and analysed on Western Blot, using the above-mentioned TF antibodies. Lysates were also analysed for β -actin expression as a loading control.

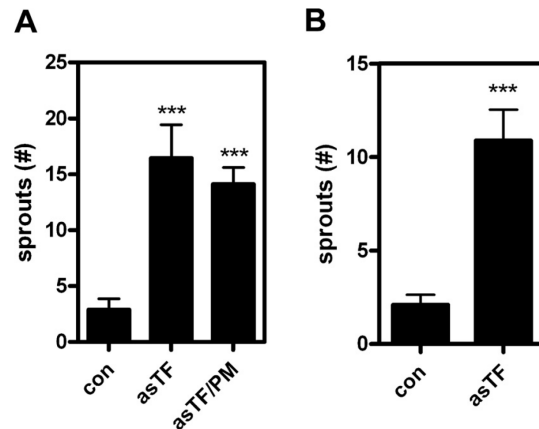


Fig. S2. asTF-dependent aortic sprouting is not caused by LPS contamination. (A) Aortic segments were implanted in solvent control-containing matrigel or asTF-containing matrigel in the presence or absence of the LPS-inhibitor polymyxin B (PM; 50 μ g/ml). (B) Aortic segments were implanted in solvent control-containing matrigel or asTF-containing matrigel and overlaid with serum-free medium. The number of sprouts was counted on day 5.

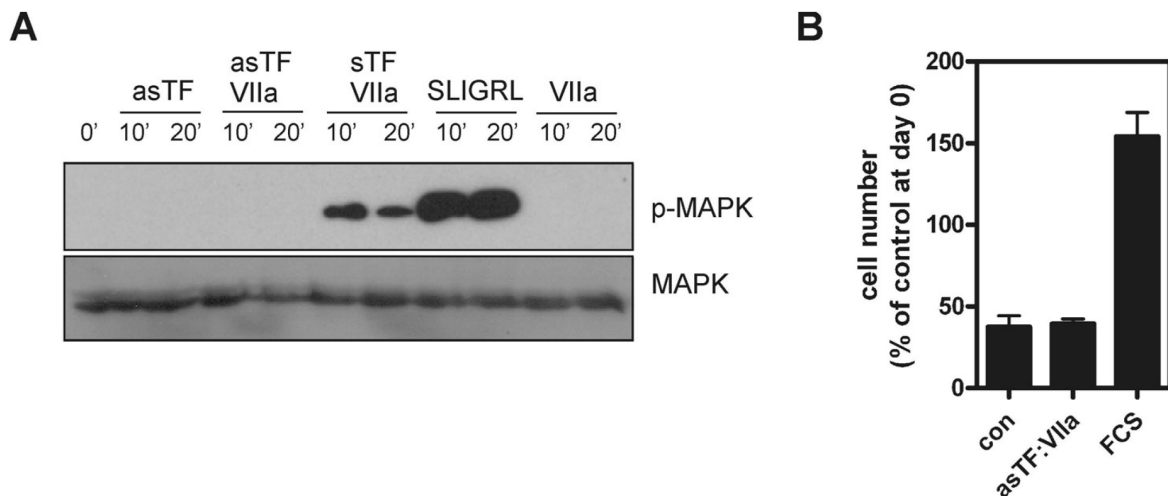


Fig. S3. asTF does not activate PAR-2 in primary HUVECs. (A) PAR-2-expressing HUVEC cells were stimulated with 100 nM asTF +/- 100 nM VIIa, VIIa alone, 100 nM truncated f1TF + VIIa, or SLIGRL (100 μ M). MAPK phosphorylation was determined by Western Blotting. (B) HUVEC cells were serum starved and stimulated with asTF + VIIa, or 15% FCS. Cell proliferation was assessed using MTT assays.

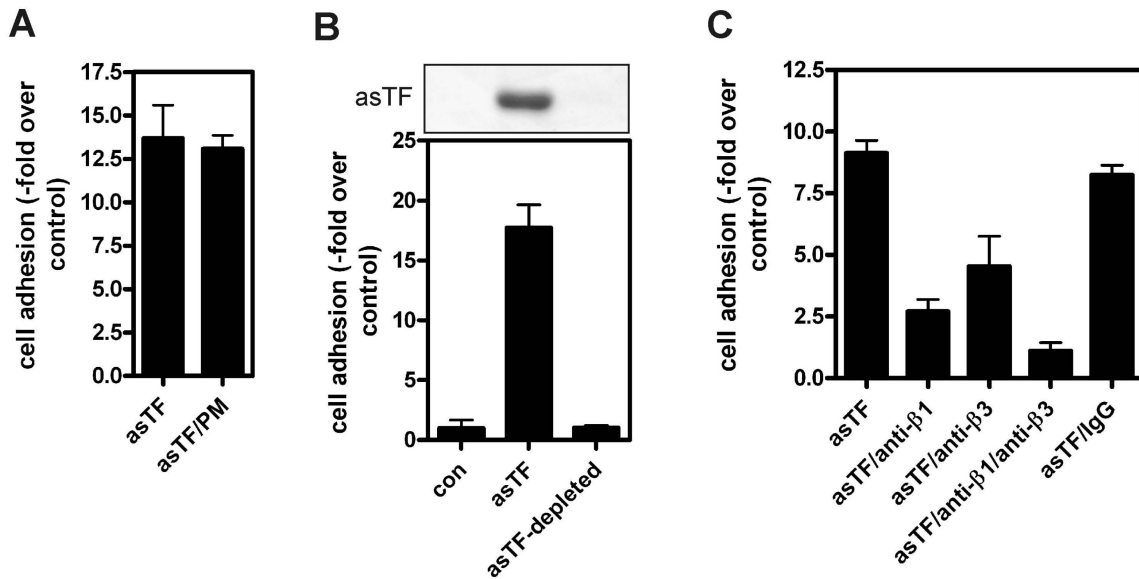


Fig. S4. Specific binding of human and mouse endothelial cells to asTF. (A) Cells were left to adhere to BSA- or asTF-coated wells for 4 h in the presence of PM. (B) asTF preparations were depleted with nickel-NTA or control beads. The supernatant was used to coat tissue culture wells. ECRF cells were seeded and adhesion was determined after 4 h. Depletion was verified on SDS-page using Coomassie staining. (C) MEECs were treated with 50 $\mu\text{g}/\text{mL}$ anti-mouse $\beta 1$, $\beta 3$, or control antibody and seeded in asTF-coated wells. Adhered cells were counted after 4 h.

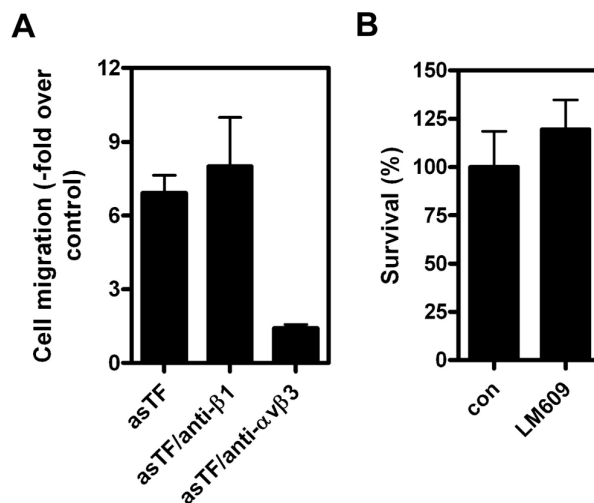


Fig. S5. $\alpha\text{v}\beta 3$ -blockade inhibits endothelial HUVEC migration, but not cell survival. (A) Transwell inserts were coated with BSA (negative control) or 50 $\mu\text{g}/\text{mL}$ asTF. Endothelial cells were preincubated with β integrin-blocking antibodies, seeded into asTF-coated transwell inserts and left to migrate for 5 h. (B) ECRF cells were incubated with LM609 in suspension to mimick migration in a transwell system. Survival was determined after 5h using an MTT assay.

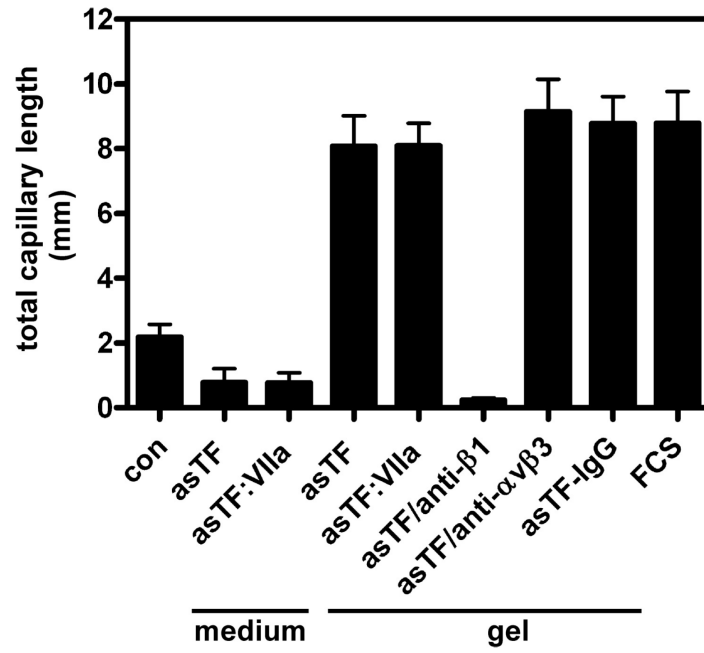


Fig.S6. asTF enhances β 1-dependent endothelial capillary formation. (A) HUVEC cells were seeded on matrigel supplemented with solvent control or 100 nM asTF after appropriate pre-incubation with β integrin blocking antibodies. Alternatively, asTF was added tot the medium containing the cells and the mix was added onto a matrigel layer without asTF. Total capillary length was quantified.

